Fuel Processing Technology 158 (2017) 255–263, http://dx.doi.org/10.1016/j.fuproc.2017.01.015

Evolution of chars during slow pyrolysis of citrus waste

Roberto Volpe[1,2*], José Miguel Bermúdez Menendez[2], Tomas Ramirez Reina [3], Antonio Messineo[1] and Marcos Millan[2]

[1]Facoltà di Ingegneria e Architettura, Università degli Studi di Enna "Kore", Cittadella Universitaria, 94100, Italy.

[2]Department of Chemical Engineering, Imperial College London, London SW7 2AZ, UK.

[3]Department of Chemical and Process Engineering, University of Surrey, Guildford, GU2 7XH, United Kingdom

Abstract

Conversion of agro-wastes into energy can be key to a circular-driven economy that could lead to models for sustainable production. Thermochemical processing is an interesting alternative for the upgrading of agro-wastes to energy. However, owing to the complex and largely unknown set of reactions occurring during thermal breakdown, to ensuring consistent quality of the final products is still a goal to achieve at industrial level. The present study investigates the evolution of solid products of pyrolysis, to gain some insights in these complexities. Chars derived from slow pyrolysis (200-650 °C) of citrus pulp in a horizontal reactor have been characterized by means of Fourier Transform Infrared spectroscopy (FT-IR), X-Ray Diffraction (XRD), Thermo Gravimetric Analysis (TGA) and Scanning Electron Microscopy (SEM). Results are discussed also in light of similarities with coal thermal breakdown.

At temperatures below 300 °C, changes in solid matrix are mainly due to breaking of aliphatic compounds. Significant changes in char structure and behavior then occur between 300 °C and 500 °C mainly related to secondary char-tar reactions. Above 500 °C, changes appear to occur mainly due to recombination reactions within matrix, which thereby becomes progressively less reactive.

Keywords: citrus waste, pyrolysis, char reactivity, downdraft gasification

*Corresponding author. Tel: +39 0935 536448; Fax: +39 0935 536951

E-mail address: roberto.volpe@unikore.it (R. Volpe).

Introduction

During the past 200 years, several methods have been proposed to efficiently gasify biomass. Different types of gasifiers potentially suitable to the different types of biomass, desired power and general conditions have been designed. Downdraft and updraft gasifiers are more suitable to small scale applications [1] and hence particularly desirable in rural areas where conversion to energy of abundant agro waste would offer a significant support to local economies while contributing to solve existing disposal issues [2].

Despite gasification has been known for a long time, although extensive research effort and significant incentive schemes have been implemented in several countries in order to support its industrial and commercial development, current lack of fundamental knowledge on biomass thermal breakdown still impedes the widespread of the technology [3,4].

The gasifying section of downdraft set-ups normally follows a pyrolysis stage in which biomass experiences increasing temperatures in a non-oxidative environment to break down into a solid carbonaceous material (char) and a hot mix of reactive vapors and non-condensable gases. The extent and type of the numerous reactions occurring within the hot fluid and between the fluid and the solids is highly dependent on the system set-up [5,6]. In moving bed systems, such as downdraft gasifiers, a relatively tall stack of chipped or shredded, typically inhomogeneous, biomass is piled up to slowly undergo thermal breakdown as temperature rises towards the gasification section. While solids move downwards through an increasingly hot bed, they experience different fates depending on the sequence of events that they undergo. The complexity at hand is exacerbated by significant heat and mass transfer limitations [7,8] as well as synergistic effects among the macro-constituents of ligno-cellulosic feedstock [9, 10].

In summary, efficient gasification of chars that evolve out of the pyrolysis stage of a downdraft set-up, largely depends on the specific, reactor's related, pyrolysis process that the chars have come out of [11].

Several authors have studied the evolution of chars in different type reactors: Zhao and co-workers [12] investigated the effect of pyrolysis temperature on char structure in an entrained flow reactor and found that pyrolysis between 500 and 900 °C resulted in ring condensation, which produces large aromatic ring systems containing six or more fused benzene rings. Song and coauthors [13] recently investigated the reactions among fresh coal and biomass tar with biomass chars to find that the aromatic structures in tar are more reactive with char than the non-aromatic structures, especially at temperatures above 800 °C. Xin and coauthors [14]

observed how dehydration due to cleavage of intra- and inter-molecular hydrogen bonds (H-bonds) was the primary reaction in pyrolysis of cellulose at temperatures below 300 °C and that above 300 °C dehydration occurred principally inter-molecularly along with decarbonylation, ring-opening and aromatization. In a recent study, the present authors have investigated the pathways that influence the reactivity of chars produced in a horizontal batch set-up simulating the pyrolysis stage of a downdraft gasifier [15]. While that work highlighted how chars evolve depending on the evolution of C and H in solids, further investigation is required to continue develop the argument and shed some additional light into the factors that govern the physical and chemical characteristics of solid products of pyrolysis especially at temperatures between 300 and 650 °C.

The present study tackles this issue, by providing a FT-IR, XRD, TGA and SEM characterization of pyrolysed lemon and orange pulp in search for clues on reactions among volatiles and solids and within the solids themselves during thermal decomposition. The results are discussed also in light of early research on coal. As reported in previous works [6,15], the comparison between coal and biomass thermal breakdown deserves investigation and the subsequent analysis will attempt at highlighting similarities. The study is also intended to support operators who look for indications to design real scale set ups and set operational parameters of existing reactors.

Materials and methods

System Set-Up

A horizontal fixed-bed type reactor, derived from the standard Gray-King (GK) assay test on coal was purposely modified to conduct pyrolysis tests. The reactor design and full details of set-up are described in [16,17]. Briefly, the system consists of a quartz-made cylindrical reactor 340 mm long and 20 mm i.d. closed at one end. A special quartz cap equipped with an 8 mm i.d. quartz inner tube allows a flow of inert gas through the feedstock to sweep volatiles away into a cold trap (mix of glycol, dry CO_2 and water bath kept at -27 °C) used to collect condensable products for mass balances.

Sample preparation

Peel waste from lemon, “Femminello” variety, and blonde orange, “Tarocco” variety, were collected as a wet pulp, right after being processed at factory located in Messina province, Sicily. The pulps were oven dried for 48 h at 60 °C and then 6 h at 105 °C to get rid of moisture. Lemon and orange pulp (LP and OP) showed respectively 83.7 % and 78.9 %

moisture by weight (as received basis). LP contained also approximately 7.5 % by weight (%w/w db) of seeds while no seeds were present in OP. Dried LP and OP were milled and again oven dried for 12 h prior to grinding and sieving to < 850 μm particle size. The feedstock was then oven dried again at 105 °C and then sieved to select particle size range between 200 and 850 μm and then pyrolysed in order to produce the chars for subsequent analyses.

Test Run

A series of pyrolysis experiments (150 °C – 650 °C peak temperatures) have been carried out under a flow of 1.5 L min^{-1} of Nitrogen (Airliquide 5.0 Alphagas 1); a detailed description is provided on [17]. Approximately 10 g (db) of sample were heated to the desired peak temperature at 50 °C min^{-1} heating rate and held at peak value for 30 minutes. Gas residence time was calculated to be approximately 3.3 s. Bio oils were condensed in a cold trap held in a thermostatic bath kept at -27 °C while non-condensed gases were filtered and vented out safely. At end of run, chars were left to cool naturally to room temperature and collected for further analyses. Char yields (M_{char}/M_{raw} %w/w db) were calculated to compare results obtained in previous studies only with the purpose of validating the runs. Runs showing char yields out of a ± 5% error range were repeated. Neither bio-oil nor gases were analyzed in the present study.

Analytical determinations

Proximate analyses were conducted on raw materials, as well as chars, in a TA Instruments Discovery TGA, Q50. Moisture content (MC), volatile matter (VM), and ashes of solid samples were determined according to the following thermal program:

1) 20 °C/min ramp to 105 °C in N_2, hold time 30 min to eliminate and determine any residual MC;

2) 15 °C/min ramp from 105 °C to 900 °C in N_2, hold time 7 min to determine VM;

3) 15 °C/min cooling down to 500 °C in N_2;

4) 15 °C/min ramp to 900 °C in air and isothermal for 10 min to determine ash content.

Fixed carbon (FC) was evaluated by difference via the following formula:

$$FC = M_i - MC - VM - Ash \quad (1)$$

where all numbers are expressed in grams and M_i indicates the original ‘as received’ mass of sample.

Ultimate analyses were performed using a CE Instruments Flash EA 1112 analyzer at Medac Ltd laboratories in Woking UK. Higher heating values (HHV) were evaluated according to the CEN/TS 14918 standard by means of a LECO AC500 calorimeter.

FT-IR study was carried out on a Perkin Elmer FT-IR 100 spectrometer. The spectrometer was set to work in transmission mode. Background subtracted spectra were collected at room temperature by co-adding 64 scans at 4 cm^{-1} resolution. The data were baseline corrected using Spectrum 10™ software.

The evolution of aromaticity in samples was calculated as the ratio I_{ar}/I_{al} between the intensities at:

- I_{ar} wavenumber associated to the stretch of C=C bonds (νC=C), and
- I_{al} wavenumber associated to the C-H stretch in aliphatic bonds (νCH_{al})

X-ray diffraction (XRD) analysis was performed on an X'Pert Pro PANalytical. Diffraction patterns were recorded with Cu Kα radiation (40 mA, 45 kV) over a 2ϑ-range of 5 to 60º and a position-sensitive detector using a step size of 0.05º and a step time of 120 s. The XRD patterns were further processed using the accompanying software in the equipment, X'PertHighscore Plus.

Finally, SEM micrographs were taken using a JEOL JSM6400 scanning electron microscope.

Results and discussion

Table 1 presents proximate and ultimate analysis of the samples investigated. Data show the expected decrease in VM with temperature and subsequent increase of FC and C. H shows limited reduction up to 300 °C to then decrease significantly above that temperature.

Table 1. Proximate and Ultimate analysis of Lemon Pulp and Orange Pulp chars. Numbers in sample names stand for the peak temperature they were obtained at in the reactor. All values are given in %w/w daf except for ash which is given in %w/w db.

	Proximate Analysis			Ultimate Analysis				HHV
	VM%	FC%	Ash%	C (%)	H (%)	N (%)	O(%)	(MJ kg^{-1})
LPRAW	75.1	24.8	2.0	47.7	5.2	1.3	45.5	18.4
LP200	69.6	30.3	3.2	52.2	5.2	1.4	40.9	21.0
LP250	65.6	34.3	3.6	57.9	5.3	1.8	34.8	23.2
LP300	57.0	42.9	3.5	63.9	4.8	1.9	29.2	26.3
LP335	50.0	49.9	3.7	68.0	4.4	2.0	25.4	28.7
LP400	40.6	59.3	4.7	70.2	3.6	1.7	24.3	30.4
LP500	37.3	62.6	6.9	76.0	2.7	1.9	19.2	31.2

LP650	25.7	74.2	6.8	79.9	1.8	1.7	16.4	30.9
OPRAW	71.0	28.9	2.5	48.5	5.2	1.1	45.1	18.1
OP200	71.8	28.1	2.1	53.0	5.2	1.2	40.5	21.4
OP250	59.8	40.1	2.1	57.5	4.8	1.4	36.1	23.3
OP300	50.3	49.6	3.4	64.5	4.6	1.7	29.1	26.7
OP325	48.7	51.2	3.6	68.7	4.3	1.9	25.0	28.7
OP400	40.4	59.5	4.8	71.8	3.6	1.7	22.6	31.2
OP500	38.4	61.5	4.9	77.6	2.8	1.7	17.7	31.8
OP650	27.6	72.3	7.9	84.0	1.8	1.3	12.7	31.3

FT-IR

Figure 1 shows the FT-IR patterns of samples while Table 2 reports the principal components associated with the different wavenumbers relevant to present study [18,19].

Table 2. Components in Biomass and Chars and assignment to wavenumbers.

Wavenumber (cm^{-1})	Assignment
1050	multiple C-O-R stretching (νC-O-R)
1550 - 1605	C=C stretching from aromatic skeletal vibration (νC=C)
1720	C=O carbonyl stretching (νC=O)
2920	C-H stretching (νC-H_{al})
3000-3500	O-H hydroxyl stretching (νO-H)

The patterns show that thermal treatment produced clear changes in the chemical functionalities and therefore in the chemical composition of the chars for both feedstocks. Remarkably, the intensity of the hydroxyl groups, of the C-H stretching associated to aliphatic compounds and the carbonyl band C=O decreased with increasing temperature. All of these features gradually disappear and, in particular, at 650 °C, samples show very limited residual functionalities especially in OP. The band ascribed to C-O-R functions evolves following the same trend with clear intensity depletion though it does not fully disappear with increasing severity of thermal breakdown. On the other hand, the bands attributed to aromatic compounds appear to remain after the thermal treatment to practically disappear only for 650 °C samples. However, for both LP and OP, this band is shifted towards lower frequencies

(from 1605 to 1550 cm^{-1}) as severity of process increases, indicating a change in the chemical environment of the C=C bonds that should be linked to some degree of chemical reorganization and graphitization as will be discussed in the following sections of the work.

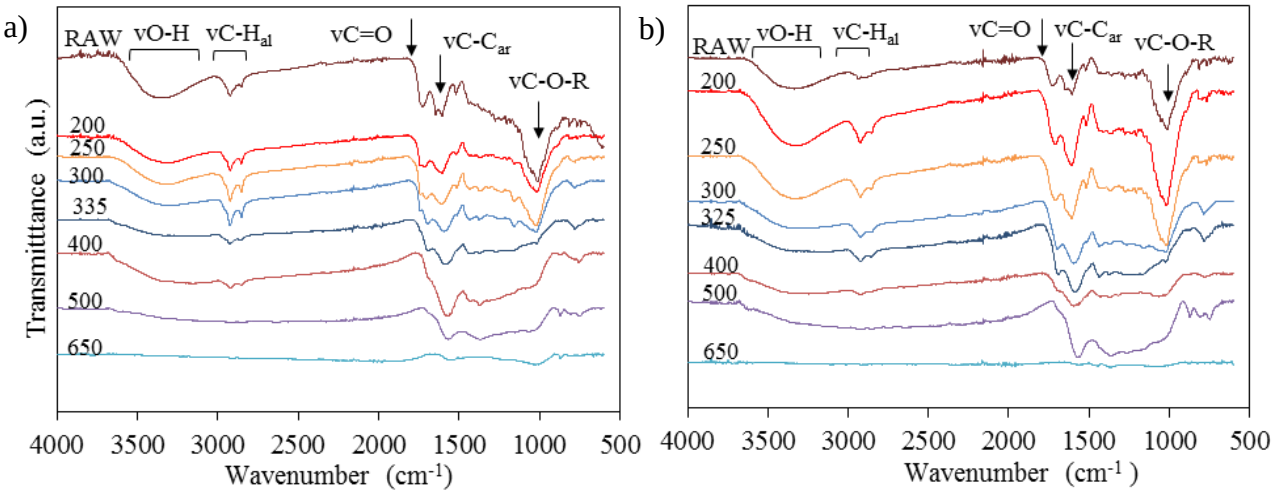


Figure 1. FT-IR patterns for LP (a) and OP (b)

As expected, and also confirmed by ultimate analysis, the plots show a distinct reduction of O-H, C=O and C-O-R chemical functionalities, which could be due to the decomposition of alcoholics groups, ester, carboxylic acid, aldehydes, etc. In addition, the aliphatic compounds tend to gradually disappear while the aromatic structures remain (although modified) with increasing severity of process. This findings are backed up by results described in [12,14]. And also by early discussion on coal. In the 'Pyrolysis' chapter of 'Chemistry of coal conversion' [20], Peter Solomon and David Hamblen describe how, at low temperatures (200-250 °C), aromatic ring structure undergo limited rearrangement while break down of aliphatic structures results in CO_2 from carboxyl and H_2O from hydroxyl groups. In the present case, a shift in aromatic band starts at 300 °C and above, for both samples, but the change is slightly more prominent in LP which also shows an aromatic peak at 650 °C (not present on OP).

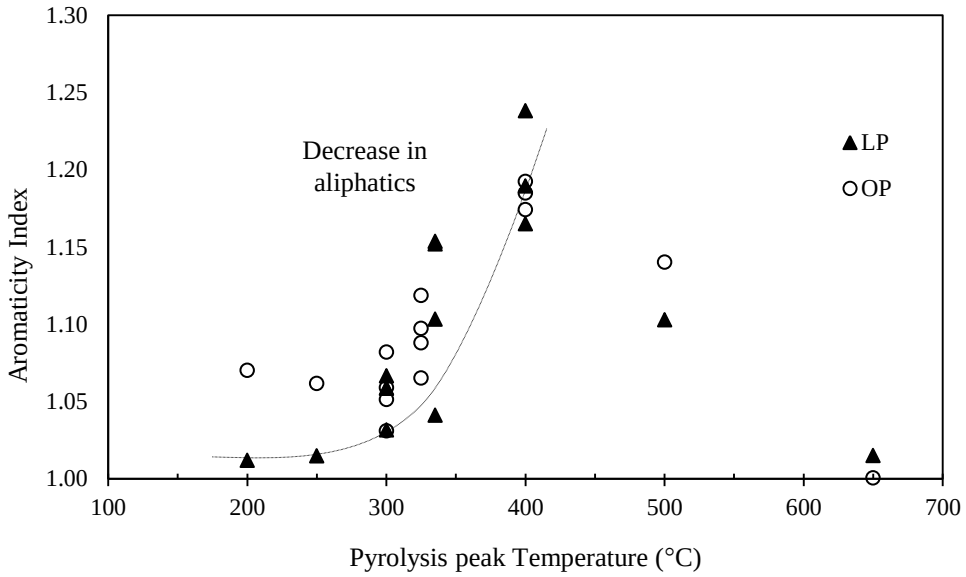


Figure 2. Index of Aromaticity defined as the ratio I_{ar}/I_{al} plotted vs. pyrolysis peak temperature. Where I_{ar} is the wavenumber associated to the stretch of C=C bonds (νC=C), and I_{al} is the wavenumber associated to the C-H stretch in aliphatic bonds (νCH_{al}).

The Index of Aromaticity, plotted vs. Pyrolysis peak temperature on Figure 2, offers elements for further discussion. Before undergoing thermal breakdown, raw matrix contains both aliphatic and aromatic compounds (mainly in lignin). When temperatures rise, between 300 and 400 °C, pyrolysis transforms woody biomass into a tarry vapor containing a mix of complex compounds, non-condensable gases and heavier hydrocarbons [21]. Picking on relevant discussion from [20], it may be inferred that, similarly to what happens to coal, up to 400 °C, the hot tarry vapors described in [21] and lighter hydrocarbons, are initially released from solids preferentially due to breaking of the aliphatic compounds. The fluid then evolves 1) by polymerizing on or 2) by cracking upon contact with hot solids. This explains the reduction of aliphatic compounds shown on Figure 1 and the increase in Aromaticity index shown on Figure 2. This finding is also in line with what reported on [12] for pyrolysis of biomass in an entrained flow reactor for temperatures above 500 °C.

At higher temperatures (at and above 400 °C) the less intense signal in FT-IR is related to aromatics undergoing condensation reactions and forming more rigid structures closer to graphite. That explains the progressive shift of aromatic peaks to smaller wavenumbers in Figure 1. This is confirmed by subsequent XRD analysis and also by reduced reactivity of chars at and above 400 °C described in the following sections.

Notably, between 300 and 400 °C, OP and LP show a clear scatter in the degree of aromaticity. The apparent uncertainty of those data is deemed related to the uncertainty of the actual fate of evolving tars within the solid matrix at a temperature around which the production of heavier compounds vs. light hydrocarbons approaches its highest degree [15, 17, 22]. In [21], Boon and co-workers describe how the solid carbohydrate fragments that are left behind during volatilization in pyrolysing cellulose, provide 'condensation sites' that prevent further volatilization of tarry fluid. In order to react with solids, tars would need to reach the solid surface or diffuse into the solid pores, and this appears to be the slow step in the process. Again, we may highlight significant similarities with coal.

In coal liquefaction experiments, tetralin is used as an H donor to stabilize fragments resulting from thermal cleavage of bonds. In [24], Hershkowitz proposes a mechanism according to which after thermal breakdown, donatable H in tetralin either stabilizes fragments or recombination reactions occur. There, if the rate of use of tetralin is high, physical limitation for tetralin to diffuse through the evolving porous matrix shows to be the limiting factor. In the present case, a vapor (tar) evolves from and can condense on a solid. When vapors are produced at higher rate (between 325 and 400 °C), the condensation reactions occurring between tars and chars depend on the physical path that vapors take around and within evolving particles. Physical contact may be limited if particularly small and tortuous porosity is generated in evolving chars.

In Figure 3, H/C atomic ratio is plotted against O/C. Both feedstocks show remarkably similar results at all the analyzed temperatures, thereby supporting the assumption that, as tars evolve rapidly from solids between 325 and 400 °C, the elemental composition of solids is similar, but the way the matrix gets rearranged depends on a series of factors mainly controlled by the amount of physical tar-char interactions occurring.

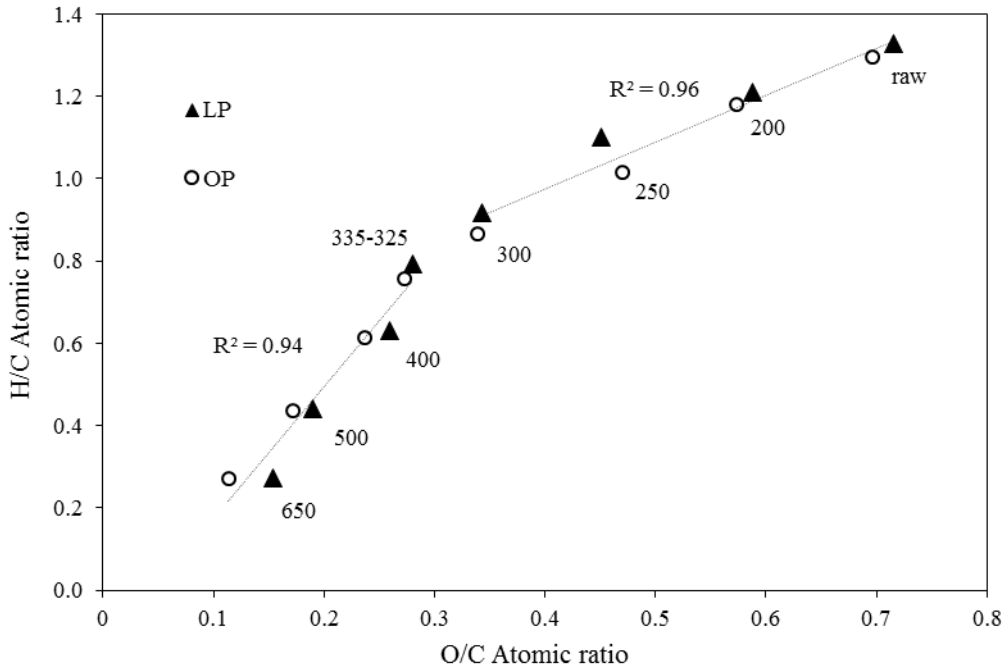


Figure 3. H/C vs. O/C atomic ratios.

Figure 3 also shows that as temperature increases, both H/C and O/C decrease consistently showing a good linear fit and very little difference between feedstocks. Notably, there is an evident change in rate of evolving O/C and H/C ratios between chars obtained up to 300 °C and chars obtained at and above that temperature. Furthermore, up to 300 °C, H/C decreases at approximately the same rate as O/C, then, at and above 325 °C, H/C starts decreasing approximately 3 times faster than O/C. This represents a further confirmation of previous findings reported on [25] where the authors highlighted the role of hydrogen in the evolution of products during thermal breakdown of biomass in a similar set up. There, a faster decrease of hydrogen in solids, occurring above 300 °C, was deemed responsible of a fast change in solids physical properties.

FT-IR patterns also show this, and in fact OP char at 650 °C does not present any significant FT-IR feature, which means that there is very limited presence of chemical functionalities (at least any chemical group active in IR), while it may be observed that LP650 conserves some aromatic groups as potential reactive sites. This observation correlates well with the XRD results in terms of the degree of graphitization as described in the following section.

X-ray diffractograms

The X-ray diffractograms of the feedstocks and the chars produced at different pyrolysis temperatures are shown in Figure 4. Again, both feedstocks show similar behaviors. The raw materials present a slight peak at $2\vartheta \sim 16^{o}$ and a broad peak at around $2\vartheta \sim 22^{o}$. These signals correspond to the crystalline structure of cellulose, which appears to be lost as the temperature rises [19, 26]. These peaks are only observed for temperatures lower than 300 ºC and cannot be distinguished at 300 ºC. This suggests that from 300 °C cellulose has reacted or lost its crystalline structure.

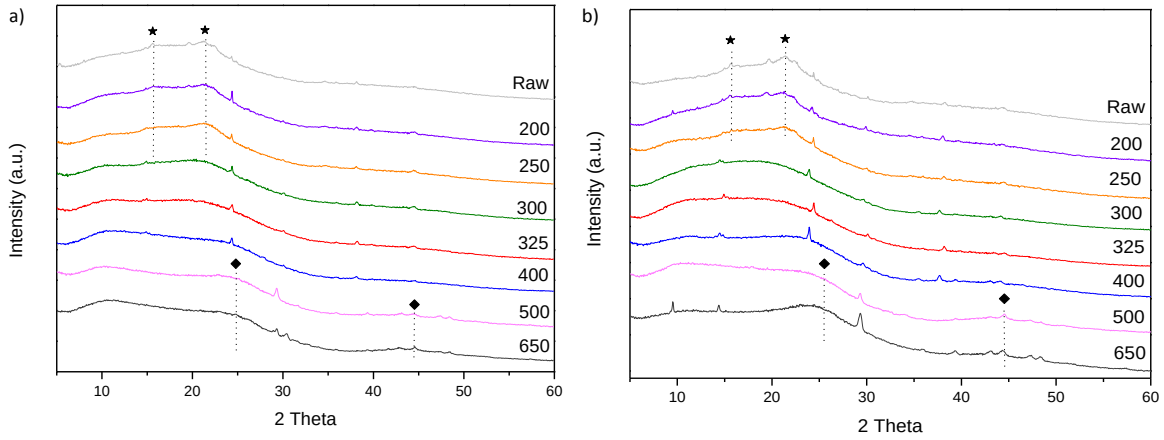


Figure 4. XRD patterns of the original feedstock and the chars produced at different pyrolysis temperatures from: a) LP; and b) OP. (*****) cellulose and (♦) graphite.

At temperatures lower than 500 ºC, samples show little differences in their crystalline phases. However, when temperature reaches 500 ºC, a broad peak at $2\vartheta \sim 26^{o}$ and a small peak at $2\vartheta \sim 44^{o}$ (500 and 650 °C samples only) can be observed. These signals seem to correspond to the incipient formation of graphitic structures, typical of pyrolysis process. As devolatilisation proceeds, carbon content in solids increases as shown in Table 1. Less reactive carbon remains in the matrix due also to the above mentioned polymerization and cracking reactions [15]. Note that volatiles can also be cracked in active catalytic centers originated by surface defects or the inorganic content of the biomass, especially Na and K [27, 28].

The unreleased carbon originally present in the matrix and/or the deposited carbon formed by secondary reactions become more graphitic (i.e. more structured and less amorphous) as temperature and reaction time increase above 400 °C. However, the relatively low temperatures and limited hold time at peak value may be deemed responsible for the general relatively low graphitic structure of the chars, as can be concluded from the low intensity of

graphite signals. Note that OP chars produced at 500 and 650 °C present some clearer graphite signals than those of LP. However, patterns are quite similar to those from activated carbons, which are predominantly amorphous carbonaceous structures [29, 30].

Earlier work on biomass and on coal may provide grounds for further discussion. In [20] the pyrolysis of coal is described as a depolymerization and thermal decomposition of functional groups with the products competing for donatable hydrogen. In [15] and in [25], the release of hydrogen during thermal breakdown, occurring more prominently above 325 °C in the same set-up, was correlated with the loss of reactivity of carbon and the reduction in calorific value of the chars. The present results corroborate previous arguments and give rise to further information on the rearranging of carbon in the biomass matrix as volatiles are released from, and in turn react with, solids at and above 325-335 °C. Remarkably, the graphitic content of the char appears more intense in OP than in LP. Thus the OP samples are expected to show lower reactivity than LP ones.

TGA

Figure 5 presents TG and DTG curves for OP and LP chars under analysis. The curves show a distinct separation mark among three groups of chars both for Lemon and Orange feedstocks: i) Raw-250 °C; ii) 300-400 °C; iii) 500, 600 °C. When heated in an inert environment, chars obtained at 200 and 250 °C largely maintain the same behavior as raw feedstock. Also, DTG curves show that substances volatized in TGA up to 330 °C may be largely divided in two classes: 1) volatiles which are released with relatively low consumption of energy and 2) volatiles which require temperature in TGA to rise to 330 °C to be volatized.

In particular, we may notice a sharp increase of the rate of volatilization (DTG) occurring just above 200 °C for raw feedstock and at slightly higher temperature for 200 °C char. This lower-temperature peak disappears on chars obtained at and above 250 °C. This first sharp peak may be related to what Kilzer and Broido called ‘dehydrocellulose’: the endothermic reactions which occur when cellulose is heated in the range of 200-280 °C [31]. When heated slowly up to 200 °C, cellulose was reported to release mainly H_2O, and then to start releasing CO and CO_2 when temperature was risen up to 250 °C, meanwhile unsaturated C-C bonds are left in solids [32]. This is also confirmed by the XRD spectra in Figure 4, which show no apparent crystallinity related to cellulose in samples pyrolysed at and above 250 °C.

When temperature is further increased in the TGA, the three samples (Raw, 200 and 250 °C chars) show a prominent peak in DTG occurring at very near 330 °C for both feedstocks. Notably, this peak occurs quite sharply at a remarkably narrow temperature band (328-332 °C) and does not show any shift in temperature as severity of pyrolysis increases up to 250 °C.

It should also here be remarked that the chars under analysis have been obtained in a set-up which significantly favors secondary reactions. The present data then signifies that the substances volatized up to 250 °C are swept away from the reactor after little or no reaction with the remaining chars, thereby confirming what stated in [32] where authors assumed that mainly H_2O, CO and CO_2 are released up to 250 °C.

Further explanation on products evolution is also provided by FT-IR patterns. O-H band appears with evident intensity on both OP and LP chars obtained to up to 250 °C and then significantly reduced on 300 °C chars and above. The stretch band related to aliphatic C-H, on the contrary, appears with significant intensity on raw feedstock and on all chars obtained up to 400 °C. It may be inferred that the second peak in DTG (the one at 330 °C) is related to the breaking of the aliphatic bonds within the matrix.

Moreover, by looking at what happens to chars obtained at 300 – 400 °C, it may be noticed that the 330 °C DTG peak is a) clearly broaden and less intense and b) shows an evident shift towards higher temperatures for both OP and LP. This also confirms what discussed on FT-IR patterns and aromaticity index. As temperature is risen above 300 °C in the GK reactor, the aromatic compounds present in the parent feedstock start to rearrange while the tarry fluids evolving from solids react with the solids themselves in a series of reactions dependent on a numerous set of variables which, altogether, determine a progressive stabilization of the thermally decomposing material. While this complex set of phenomena is responsible for the broadening of the DTG curves for samples obtained at and above 300 °C, the shift in maximum DTG confirms that the matrix becomes progressively more stable. In particular, LP300 DTG peak is significantly higher than that of OP300, while little differences are to be noticed in chars obtained at 325-335 °C and 400 °C. This is probably be related to specific fate undergone by the aliphatic compounds in the analyzed samples.

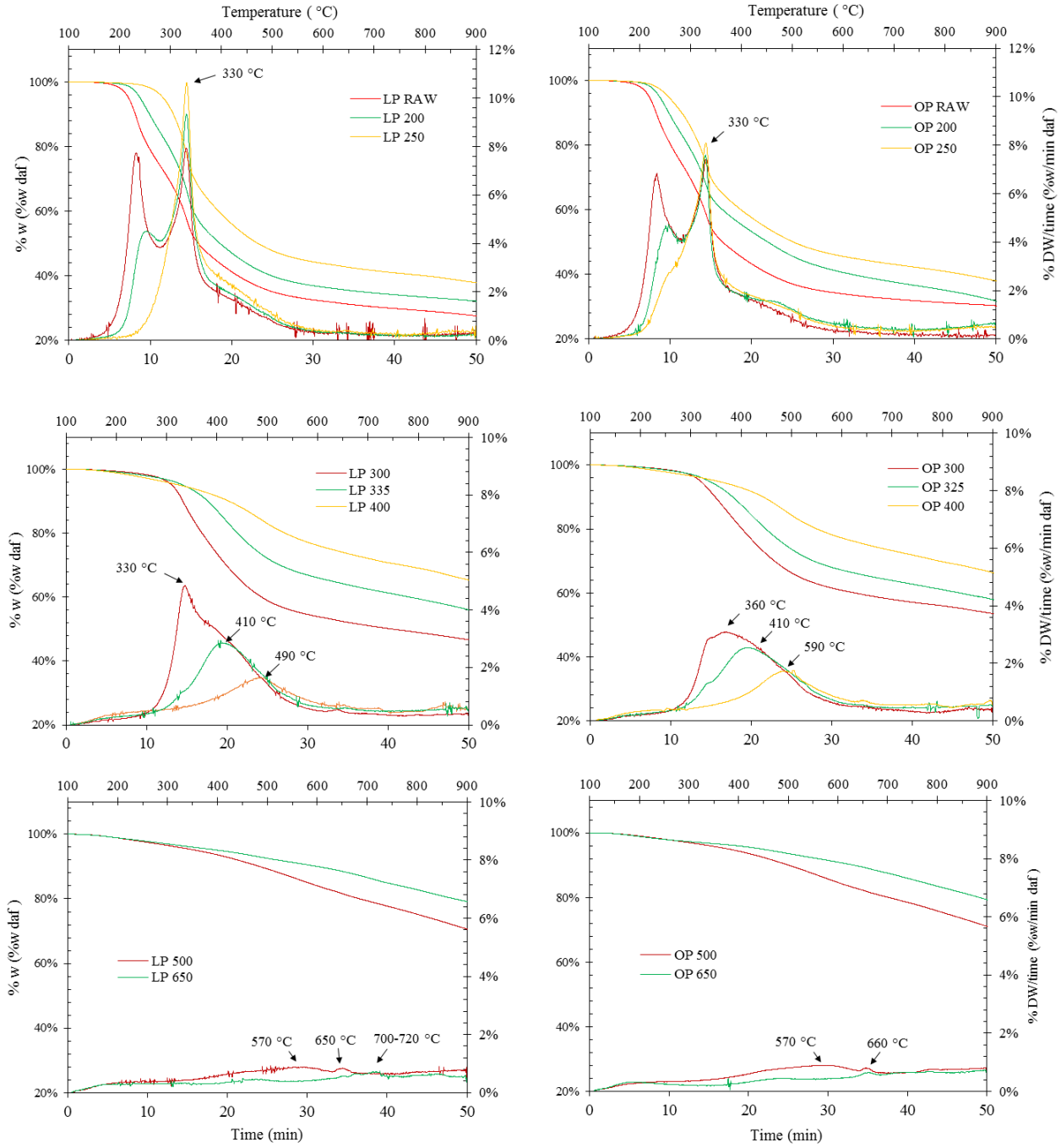


Figure 5. TGA and DTG curves of LP and OP

The observed shift in DTG peak for higher temperature chars also provides the following insights. In Figure 6, the temperature at which the maximum of DTG occurs (T_{dtgmax}) is plotted vs. Pyrolysis peak temperature ($T_{p\text{-}peak}$). The plot shows two clearly distinct areas between samples subject to pyrolysis below and up to 300 °C and samples which have experienced more severe treatments. The first ones show the clear and repeatable T_{dtmax} at 330 °C, while the other chars show higher T_{dtmax}. The evidence that $T_{dtmax} > T_{p\text{-}peak}$, is

certainly no surprise especially in the present case, where chars are obtained in a reactor that strongly favors secondary reactions, partly responsible for the loss of reactivity of solids. Nonetheless, the difference between T_{dtmax} and $T_{p\text{-}peak}$ ($\Delta T_{dtmax\text{-}ppeak}$) may provide interesting information. In Figure 6 $\Delta T_{dtmax\text{-}ppeak}$ is represented by the distance between the experimental points and the ideal $T_{dtmax} = P_{peak}$ case (represented by a dashed line in the figure). This distance is clearly related to different pyrolysis conditions experienced by feedstock in GK and, subsequently in the TGA.

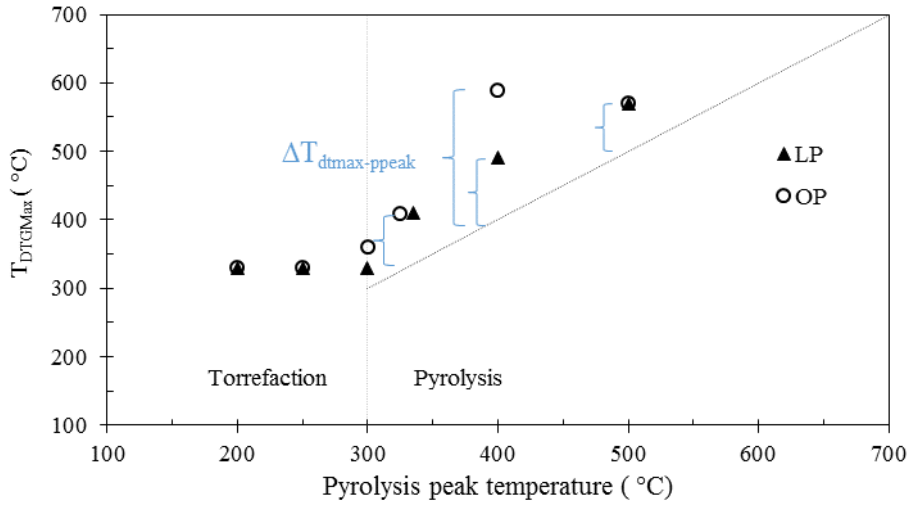


Figure 6. Maximum DTG temperature vs. Pyrolysis peak temperature

Compared to the TGA, GK set-up is clearly expected to lead to significantly more extra-particle secondary reactions responsible to progressive loss of char reactivity. Char-tar reactions and subsequent loss of char reactivity are functions of both the rate of tar production at a certain temperature and the extent and type of reactions induced by the temperature itself. In the present case, however, the loss of reactivity of chars in GK is also due to recombination reactions induced by the residence time of samples at peak temperature. Whilst further studies would be needed to decouple the role of char-tar vs. matrix recombination reactions, $\Delta T_{dtmax\text{-}ppeak}$ may be used to qualitatively represent the total loss of char reactivity related to present reactor configuration. Notably, the higher $\Delta T_{dtmax\text{-}ppeak}$ is observed between 325 °C and 500 °C: the temperature interval at which tar is released more prominently in GK set up [15, 17, 33, 34].

In addition, data plotted in Figure 6 provides further strength to the commonly known 'conventional transition line' between torrefaction and pyrolysis normally located between

280 and 300 °C peak temperatures [25]. Finally, the fact that DTG curves of the two feedstocks are very similar above 500 °C supports previous findings that demonstrated how fixed carbon formed by secondary reactions is formed mainly below 500 °C [21].

SEM

SEM images have been taken with the aim of studying the morphological properties of the chars. The evolution of structure of biomass particles during pyrolysis is a factor that can influence the chemistry of the process, and, in turn, their reactivity [35, 36]. Figure 7 shows the SEM images obtained for raw LP, pyrolysed at an intermediate temperature (300 °C) and at high temperature (650 °C), and Figure 8 shows the same images for the OP. In spite of the low heating rate used for the pyrolysis process, the morphology of both OP and LP chars differs substantially from the raw feedstock.

In general, when woody biomass is pyrolysed, chars conserve the fibrous nature of the original structure even at high temperatures and this structure is only lost when subject to high heating rates [11, 27, 36, 37]. However, in the present case, it can be clearly observed that the surface of the chars appears much more homogenous than the original feedstock. In a previous work on olive trimming and pulp, chars produced from the same horizontal reactor under similar heating rate and peak temperatures [25], the authors showed how the surface of the samples would become more homogeneous as feedstock was subject to increasing severity of slow pyrolysis. In that case, it appeared clear how the general structure of the biomass was preserved and the authors related the change in superficial appearance of samples to coating and bubbling phenomena possibly related to secondary char-forming reactions. In this case however, the original structure of feedstock appears to be lost and the treated biomass shows what may be related to a softening phase possibly linked to melting of Pectin which starts occurring at 150 °C leaving evidence still at 300 °C [38, 39]. Naturally it cannot be excluded that what is seen in present micrographs is also related to secondary charring, especially at higher temperatures. however, high VM content has already been reported to affect the chances of the biomass particles to melt [11] and coalescence of pores and softening biomass were also reported on constant pressure reactors by Pohlmann et al. in [18].

In the present case, the phenomenon seems more favored in LP, where, in Figure 7 it is clear that at both 300 °C and 650 °C the surface appears more homogeneous than that of OP (Figure 8). OP char produced at 300 °C, in fact, presents a mixed morphology of smooth

surfaces and small particles more similar to the original biomass or possibly related to secondary char depositions. This finding could well relate to the higher pectin content of LP compared to OP [40].

The development of porosity can also be affected by the mentioned softening and coating phenomena. As it can be observed, the chars produced from OP, present what appears to be a small development of macroporosity whereas in the case of chars from LP no apparent macroporosity can be observed. Naturally this is only qualitative visual evidence and any relation with gas adsorption analysis, would be useful to quantify results [41].

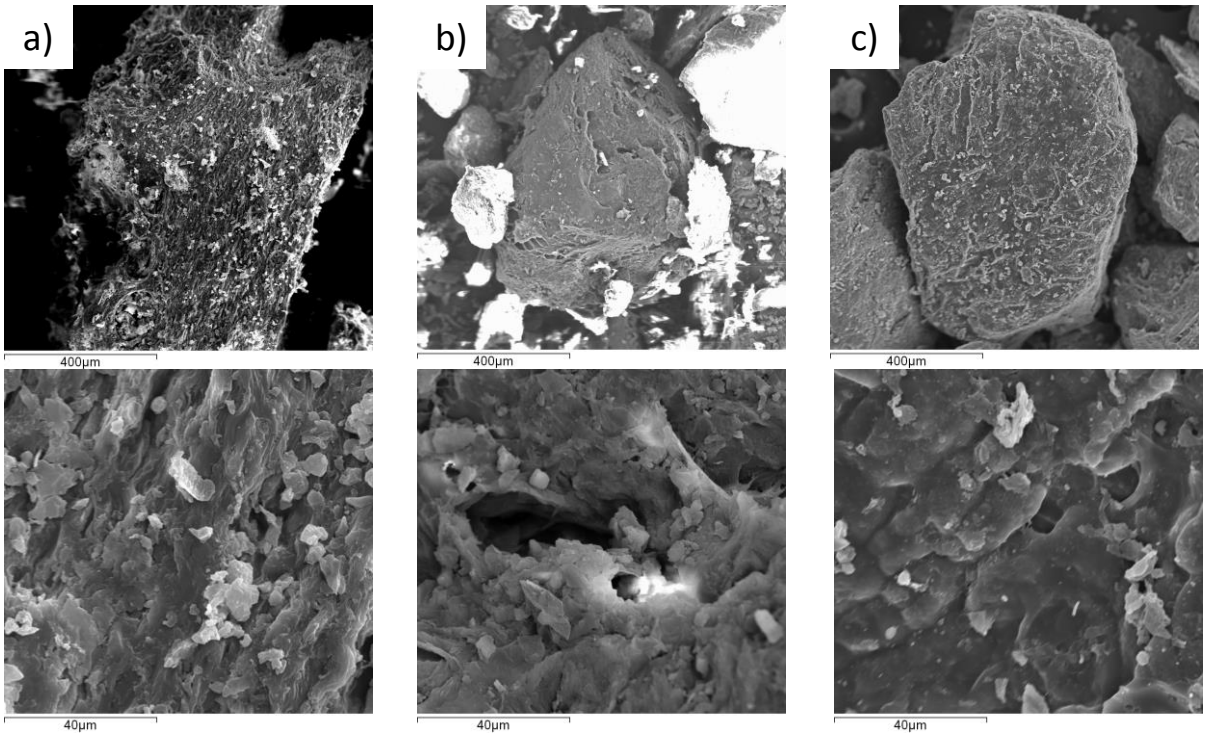


Figure 7. SEM images (100x and 1000x) of: a) raw lemon pulp; b) lemon pulp pyrolysed at 300 °C; and c) lemon pulp pyrolysed at 650 °C.

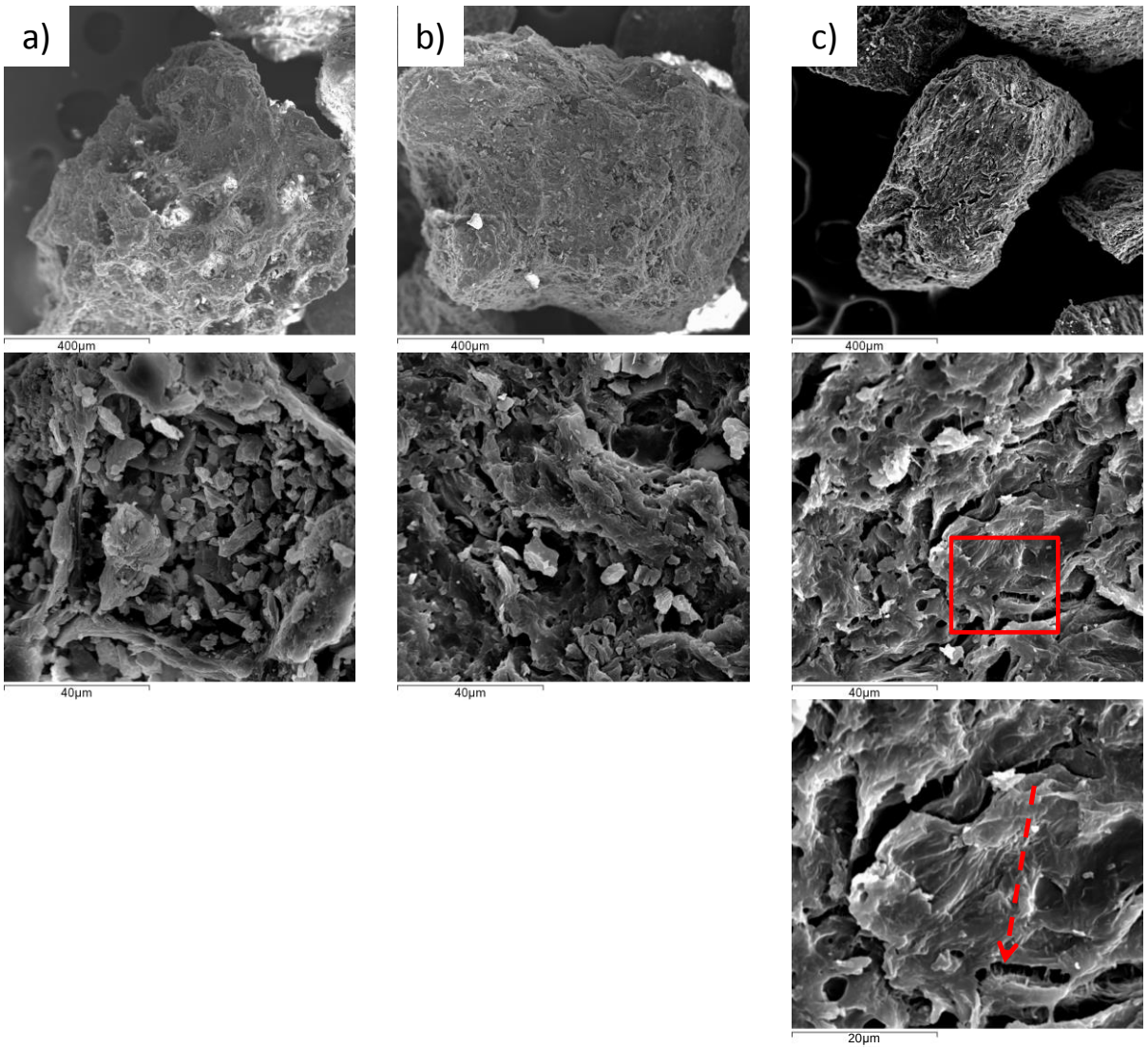


Figure 8. SEM images (100x and 1000x) of: a) raw orange pulp; b) orange pulp pyrolysed at 300 °C; and c) orange pulp pyrolysed at 650 °C.

Factors like heating rate or secondary reactions with volatiles are known to have an impact on the development of porosity. In particular, the reactions between evolving volatiles on hot solids can modify the surface of the chars. Both polymerization and cracking of tarry compounds may play a significant role. The growth of the carbon deposits can end up in pore blockage, thus reducing porosity as it may also be inferred by results in [22]. A specific evidence of secondary charring in the solids produced from OP can be observed at the highest magnification in Figure 8c. The walls of macropores (highlighted by the dashed arrow) show several fibers typically formed by carbon deposition during hydrocarbons cracking [42, 43].

The development of porosity of chars is also certainly influenced by the heating rate applied in present case. In general terms, micropores are known to be favored by slow heating, while

high heating rates give rise to the development of macroporosity due to the fast escape of volatiles [11, 43-46]. In addition, the heating rate also plays a role in the resulting particle size of the chars, since high heating rates give rise to phenomena like particle breakage (due to violent volatile releasing) or swelling. As a result, chars produced at high heating rates may present lower particle size than the original biomass [37, 44]. This would not happen when feedstock is heated slowly such as in present case, where particles appear to have preserved their size.

Conclusions

The present study highlights results of biomass slow pyrolysis experiments, also in light of early research on coal. The results sheds some additional lights in the complex pathways which govern the evolution of solids during thermal decomposition in downdraft-like set-ups which favor secondary tar char reactions. The temperature range between 300 and 500 °C is highlighted as the window within which the major changes in matrix occur due to secondary reactions. Changes occurring below or above that temperature range, up to 650 °C, appear related mainly to rearrangements of compounds within the matrix. In particular, changes occurring up to 300 °C are mainly related to the breaking of aliphatic bonds, while, changes above 500 °C appear connected to rearrangement of the aromatic structures which cause a reduction in the reactivity of solids.

Limitations to the diffusion of tar within the evolving porosity of chars become significant and play an important role when rate of tar production is high between 300 and 400 °C. A qualitative measure of loss of reactivity in solids, due to char-tar reactions and to rearrangements within matrix is represented by the difference between the temperature at which maximum DTG occurs in chars vs. the pyrolysis peak temperature at which those chars were obtained.

References

[1] Reed T.B. and Das A., “Handbook of Biomass Downdraft Gasifier Engine Systems”, The Biomass Energy Foundation Press, 1988.

[2] Messineo A, Volpe R, Marvuglia A. Ligno-cellulosic biomass exploitation for power generation: A case study in Sicily. Energy 2012;45: 613–25.

[3] Mettler MS, Vlachosb DG and Dauenhauer PJ. Top ten fundamental challenges of biomass pyrolysis for biofuels. Energy Environmental Science. 2012;5:7797-809.

[4] Kirkels A.F., Verbong G. P.J., Biomass gasification: Still promising? A 30-year global overview. Renewable and Sustainable Energy Reviews 15 2011, 471–481

[5] Gonenc S., Gibbinst J.R., Katheklakis I.E. and Kandiyoti R. Comparison of coal pyrolysis product distributions from three captive sample techniques Fuel, 1990 69, 383-390.

[6] Morgan TJ and Kandiyoti R. Pyrolysis of Coals and Biomass: Analysis of Thermal Breakdown and Its Products. Chemical Reviews. 2014;114,:1547−607.

[7] Jess A., Andresen A-K. Influence of mass transfer on thermogravimetric analysis of combustion and gasification reactivity of coke Fuel 2010 89, 1541–1548

[8] Kandiyoti R., Reply to Letter to the Editor by Sun et al. Fuel 2002 81, 975

[9] Couhert C., Commandre J.-M., Salvador S., Is it possible to predict gas yields of any biomass after rapid pyrolysis at high temperature from its composition in cellulose, hemicellulose and lignin? Fuel 2009 88, 408–417

[10] George A., Morgan T.J. and Kandiyoti R. Pyrolytic Reactions of Lignin within Naturally Occurring Plant Matrices: Challenges in Biomass Pyrolysis Modeling Due to Synergistic Effects. Energy & Fuels 2014, 28, 6918−6927

[11] Cetin E., Moghtaderi B., Gupta R., Wall T.F. Influence of pyrolysis conditions on the structure and gasification reactivity of biomass chars. Fuel 2004 83, 2139–2150

[12] Zhao Y., Feng D., Zhang Y., Huang Y., Sun S. Effect of pyrolysis temperature on char structure and chemical speciation of alkali and alkaline earth metallic species in biochar. Fuel Processing Technology 2016, 141, 54–60

[13] Song Y., Xiang J., Hu S., Quyn D.M., Zhao Y., Hu X., Wanga Y., Li C-Z. Importance of the aromatic structures in volatiles to the in-situ destruction of nascent tar during the volatile–char interactions. Fuel Processing Technology 2015, 132, 31–38.

[14] Xin S., Yang H., Chen Y., Yang M., Chen L., Wang X., Chen H. Chemical structure evolution of char during the pyrolysis of cellulose. Journal of Analytical and Applied Pyrolysis 2015, 116, 263–271.

[15] Volpe R., Messineo A., Millan M. Carbon reactivity in biomass thermal breakdown. Fuel 2016 183: 139–144.

[16] Volpe M., D'Anna C., Messineo S., Volpe R., Messineo A. Sustainable production of bio-combustibles from pyrolysis of agro-industrial wastes. Sustainability. 2014;6(11):7866-82.

[17] Volpe M., Panno D., Volpe R., Messineo A. Upgrade of citrus waste as a biofuel via slow pyrolysis. Journal of Analytical and Applied Pyrolysis. 2015;115: 66–76.

[18] Pohlmann J.G., Osório E. Vilela A.C.F., Diez M.A., Borrego A.G. Integrating physicochemical information to follow the transformations of biomass upon torrefaction and low-temperature carbonization. Fuel 2014, 131: 17–27.

[19] Nanda, S., Mohanty, P., Pant, K.K. et al. Characterization of North American Lignocellulosic Biomass and Biochars in Terms of their Candidacy for Alternate Renewable Fuels. Bioenergy Resources (2013) 6:663–677.

[20] Solomon PR and Hamblen DG. Pyrolysis. In Richard H. Schlosberg editor. Chemistry of coal conversion, New York: Springer Science+Business Media 1985 p. 121-248.

[21] Antal MJ Jr, Grønli M., The Art, Science, and Technology of Charcoal Production. Industrial Engineering Chemistry Research. 2003, 42:1619-1640

[22] Dabai F., Paterson N., Millan M., Fennell P., and Kandiyoti R. Tar Formation and Destruction in a Fixed Bed Reactor Simulating Downdraft Gasification: Effect of Reaction Conditions on Tar Cracking Products Energy Fuels 2014, 28, 1970−1982.

[23] Boon JJ, Pastorova I, Botto RE, Arisz PW. Structural Studies on Cellulose Pyrolysis and Cellulose Chars by PYMS, PYGCMS, FT-IR, NMR, and by Wet Chemical Techniques. Biomass Bioenergy 1994, 7, 25-32

[24] Hershkowitz F, Mass Transfer Effects in Coal Conversion Chemistry. In Richard H. Schlosberg editor. Chemistry of coal conversion, New York: Springer Science+Business Media 1985 p.45-64.

[25] Volpe R, Messineo A, Millan M, Volpe M, Kandiyoti R. Assessment of olive wastes as energy source: pyrolysis, torrefaction and the key role of H loss in thermal breakdown. Energy. 2015;82:119–27.

[26] Deraman M., Zakaria S., and Murshidi JA. Estimation of Crystallinity and Crystallite Size of Cellulose in Benzylated Fibres of Oil Palm Empty Fruit Bunches by X-Ray Diffraction. Japanese Journal of Applied Physics, 2001, 40: 3311-3314

[27] Manyà JJ., Ruiz J., and Arauzo J. Some Peculiarities of Conventional Pyrolysis of Several Agricultural Residues in a Packed Bed Reactor. Industrial and Engineering Chemistry Research 2007, 46: 9061-9070

[28] Volpe R, Messineo S, Volpe M, Messineo A. Catalytic effect of char for tar cracking in pyrolysis of citrus wastes, design of a novel experimental set up and first results. Chemical Engineering Transactions 2016, 50: 181-186

[29] Cao Y, Wang K, Wang X, Gu Z, Fan Q, Gibbons W, Hoefelmeyer JD, Kharel PR, Shrestha M. Hierarchical porous activated carbon for supercapacitor derived from corn stalk core by potassium hydroxide activation. Electrochimica Acta, 2016, 212: 839-847.

[30] Chong Lua A and Ting Y.. Effect of activation temperature on the textural and chemical properties of potassium hydroxide activated carbon prepared from pistachio-nut shell. Journal of Colloid and Interface Science. 2004 274: 594–601.

[31] Kilzer F.J., Broido A. Speculations on the nature of cellulose pyrolysis. Pyrodynamics 1965, 2:151–163

[32] Arsenau DF. Competitive reactions in the thermal decomposition of cellulose. Canadian Journal of Chemistry 1971, 49: 632-638

[33] Cordella M., Torri C., Adamiano A., Fabbri D., Barontini F., Cozzani V. Bio-oils from biomass slow pyrolysis: A chemical and toxicological screening Journal of Hazardous Materials 231–232 (2012) 26–35

[34] Zaror C.A., Hutchings I.S., Pyle D.L., Stiles H.N. and Kandiyoti R. Secondary char formation in the catalytic pyrolysis of biomass. Fuel, 1985, 64: 990-994.

[35] Baliga V., Sharma R., Miser D., McGrath T., Hajaligol M. Physical characterization of pyrolyzed tobacco and tobacco components. Journal of Analytical and Applied Pyrolysis 2003, 66: 191-215

[36] Fisher EM., Dupont C., Darvell LI., Commandré J.-M., Saddawi A., Jones J.M., Grateau M., Nocquet T., Salvador S. Combustion and gasification characteristics of chars from raw and torrefied biomass. Bioresource Technology 2012, 119: 157–165

[37] Li T., Geier M., Wang L., Ku X., Matas Güell B., Løvas T., and Shaddix C. R. Effect of Torrefaction on Physical Properties and Conversion Behavior of High Heating Rate Char of Forest Residue. Energy Fuels 2015, 29: 177-184

[38] Fisher T, Hajaligol M, Waymack B, Kellogg D. Pyrolysis behavior and kinetics of biomass derived materials. Journal of Analytical and Applied Pyrolysis 2002, 62: 331–349.

[39] Gropper SS., Smith JL. In Wadsworth Pub Co. editor. Advanced nutrition and human metabolism, 6th edition. Cengage Learning Inc., 2012.

[40] Sulieman AME., Khodari KMY., Salih ZA. Extraction of Pectin from Lemon and Orange Fruits Peels and Its Utilization in Jam Making. International Journal of Food Science and Nutrition Engineering 2013, 3(5): 81-84

[41] Titirici M, White RJ, Brun N, Budarin V, Dang Sheng S, del Monte F, et al. Sustainable carbon materials. Chemical Society Review. 2015;44:250-290.

[42] Monnerat B, Kiwi-Minsker L, Renken A. Hydrogen production by catalytic cracking of methane over nickel gauze under periodic reactor operation. Chemical Engineering Science, 2001, 56: 633-639

[43] Zhang T, Amiridis MD. Hydrogen production via the direct cracking of methane over silica-supported nickel catalysts. Applied Catalysis A: General 1998 167: 161-172.

[44] Brewer CE, Schmidt-Rohr K, Satrio JA, and Brown RC. Characterization of Biochar from Fast Pyrolysis and Gasification Systems. Environmental Progress & Sustainable Energy, 2009, 28 (3), 386-396.

[45] Bridgwater AV. Review of fast pyrolysis of biomass and product upgrading. Biomass and Bioenergy. 2012;38:68 -94.

[46] Sharma RK, Wooten JB, Baliga VL, Lin X, Chan WG, Hajaligol MR. Characterization of chars from pyrolysis of lignin. Fuel 2004, 83: 1469-1482.